3002–3010 *Nucleic Acids Research, 2005, Vol. 33, No. 9*
doi:10.1093/nar/gki613

DNA damage response and Ku80 function in the vertebrate embryo

Catherine L. Bladen[1], Wai K. Lam[1], William S. Dynan[1] and David J. Kozlowski[1,2,*]

[1]Institute of Molecular Medicine and Genetics and [2]Department of Cellular Biology and Anatomy, Medical College of Georgia, Augusta, GA 30912, USA

Received March 20, 2005; Revised and Accepted May 4, 2005

DDBJ/EMBL/GenBank accession no AY877316

ABSTRACT

Cellular responses to DNA damage reflect the dynamic integration of cell cycle control, cell–cell interactions and tissue-specific patterns of gene regulation that occurs *in vivo* but is not recapitulated in cell culture models. Here we describe use of the zebrafish embryo as a model system to identify determinants of the *in vivo* response to ionizing radiation-induced DNA damage. To demonstrate the utility of the model we cloned and characterized the embryonic function of the *XRCC5* gene, which encodes Ku80, an essential component of the non-homologous end joining pathway of DNA repair. After the onset of zygotic transcription, Ku80 mRNA accumulates in a tissue-specific pattern, which includes proliferative zones of the retina and central nervous system. In the absence of genotoxic stress, zebrafish embryos with reduced Ku80 function develop normally. However, low dose irradiation of these embryos during gastrulation leads to marked apoptosis throughout the developing central nervous system. Apoptosis is p53 dependent, indicating that it is a downstream consequence of unrepaired DNA damage. Results suggest that nonhomologous end joining components mediate DNA repair to promote survival of irradiated cells during embryogenesis.

INTRODUCTION

In the nucleus, interaction of an ionizing radiation track with duplex DNA causes many types of DNA lesions, the most potent of which are double-strand breaks [DSBs; reviewed in (1)]. Upon formation and detection of DSBs, cells enter DNA damage-dependent cell cycle arrest and attempt to reestablish chromosome integrity by repair of DNA DSBs. This repair may occur either by nonhomologous end joining (NHEJ) or by homologous recombination [reviewed in (2,3)]. Alternatively, and depending on the extent of damage per cell or within a tissue, a cell may self-eliminate by apoptosis [reviewed in (4)].

Our understanding of the DNA damage response in vertebrates has been gained primarily from cell culture models, which cannot recapitulate dynamic *in vivo* processes such as temporally and spatially regulated patterns of gene expression. Work described here uses the zebrafish embryo as an *in vivo* model of the DNA damage response. Embryogenesis is a particularly radiosensitive stage of the vertebrate life cycle, perhaps because of rapid cell division. Thus, for any given species, radiosensitivity during embryogenesis has significant consequences for survival of the organism in particular and for the population in general.

The current framework for understanding radiation effects on the embryo [reviewed in (5)] derives from classical experiments performed before the advent of modern molecular biological tools (6). Mammalian embryos exposed to radiation at the pre-implantation stage exhibit an 'all or none' effect, where the embryo is either nonviable or develops normally. Embryos exposed to sublethal doses of radiation have changes that are observable as a proliferative disadvantage in aggregation chimeras (7). Although the radiosensitive target is in the nucleus, the precise damage pathways have not been explored at the molecular level (8).

Exposure at later times, during organogenesis, causes tissue-specific malformations consistent with exposure during sensitive 'critical periods' of organ-specific formation or morphogenesis (6,9). These findings, together with other observations that radiation exposure at pre-implantation or organogenic stages poses little or no excess cancer risk, suggest a mechanism where self-elimination of radiation-injured cells is favored over DNA damage tolerance and repair (10,11). Indeed, this self-elimination is now known to occur by p53-dependent apoptosis (12–14). Vertebrate embryos become able to undergo apoptosis, in response to earlier genotoxic damage, only during gastrulation stages (15–17). In zebrafish, ability to undergo checkpoint-dependent apoptosis begins at ~7 h post-fertilization (hpf) (18).

*To whom correspondence should be addressed. Tel: +1 706 721 8760; Fax: +1 706 721 8752; Email: dkozlowski@mcg.edu

In contrast to self-elimination of radiation-injured cells earlier during embryogenesis, exposure at later, fetal, stages of development leads to a significant excess cancer risk. This is seen both in rodent models (11,19) and among children exposed to low dose diagnostic X-rays during the third trimester of pregnancy (20–23). Presumably, these cancers result from the survival of cells bearing chromosomal aberrations or other mutations fixed in the genome by error-prone DNA repair. The mechanisms regulating the decision between cellular self-elimination and DNA repair in the embryo and fetus remain largely unknown.

Here, we use a zebrafish (*Danio rerio*) embryo as a model system to investigate the effects of radiation on the embryo. Several features of the zebrafish embryo facilitate experimental determination of gene function during embryonic development and in response to genotoxic stress, including irradiation (24). These include optical transparency, external development, large clutch sizes and amenability to molecular, cellular and genetic manipulation (25). Although gene replacement by homologous recombination is not available in the zebrafish, gene function is easily and quickly determined by transient knockdown of gene function using antisense morpholino oligonucleotides (MOs) (26).

We have investigated the effects of ionizing radiation on the zebrafish embryo in the presence or absence of *XRCC5* gene function. *XRCC5* encodes the Ku80 protein, an essential component of the NHEJ pathway of DSB repair (27–29). This pathway requires at least four other genes: *LIG4* and *XRCC4*, which encode two subunits of a DNA ligase, *PRKDC*, which encodes the DNA-dependent protein kinases catalytic subunit, and *G22P1*, which encodes the Ku70 protein. Each of these genes has been knocked out in mice to result in a severe radiosensitivity, in some cases accompanied by other phenotypes [reviewed in (2,30)].

We show that zebrafish Ku80 mRNA specifically accumulates in regions or tissues of the embryo containing rapidly proliferating cells, including the ventricular surface of the brain and retinal ganglion cells in the developing retina. Suppression of Ku80 expression using antisense morpholino oligonucleotides sensitizes early embryos to radiation-induced, p53-dependent apoptosis. This is in contrast to wild-type embryos that do not have increased numbers of apoptotic cells at the same exposure doses. Together, these results suggest that expression of DSB repair genes plays a critical role in establishing the balance between cell survival and apoptosis in early development.

MATERIALS AND METHODS

Zebrafish methods

All experiments were carried out with wild-type Tuebingen or *brass* embryos. Breeding and staging of embryos was performed according to standard protocols (31,32). For each experiment, a single clutch containing 200 or more embryos was used, with a minimum of 20 embryos per condition. Each experiment was repeated with at least two clutches and each figure shows representative embryos from an experimental group. Irradiation (^{137}Cs) was performed using a Gammacell Exactor (MDS Nordion, Ottawa, ON, USA) at a dose rate of ~1 Gy/min. Doses were as indicated in the figures and figure legends. Dosimetry was performed using thermoluminescence dosimetry devices (Landauer Inc., Glenwood, IL, USA) irradiated simultaneously with the embryos. Each experiment included control embryos that were transported to the irradiator but not irradiated. TUNEL analysis was carried out to determine levels of apoptosis in the embryos as described elsewhere (33).

Ku80 cDNA cloning

Total RNA was isolated using the Trizol reagent (Life Technologies, Gibco BRL, USA), according to the manufacturer's instructions. First-strand cDNA was generated by reverse transcription (Omniscript™ Reverse Transcriptase for First-strand cDNA synthesis, Qiagen, Valencia, CA, USA) primed with a polyT primer and used as a template for PCR.

To identify Ku80 sequences, the GenBank database was searched for sequences similar to mammalian Ku80 using the BLAST algorithm (www.ncbi.nlm.nih.gov/blast). Four zebrafish ESTs (fi98a07, fk23b01, fk52e08, fd41d05) similar to Ku80 were identified. Ku80-specific PCR primers were designed from these sequences and an existing cDNA clone (gift from Dr P. Chang, University of Singapore). Full-length Ku80 cDNA was amplified using primers Ku80f1 (5′-GCACGAGCGGAAGCCAGCAGC-3′) and Ku80r1 (5′-ATTCAAGTTTCAGTGGCTGTT-3′), purified by agarose gel electrophoresis and cloned using the pGEM-Teasy Vector System (Promega Corp., Madison, WI, USA). The identities of cDNA clones were confirmed by sequencing both DNA strands. Additional Ku80 PCR primers Ku80f2 (5′-TGGTTTGGTGCTGTTTGGTA-3′) and Ku80r2 (5′-ACAAATAGAGGCTGCCGAAT-3′) were used for semi-quantitative RT–PCR analysis of Ku80 mRNA as described above and shown in Figure 3A.

Whole-mount *in situ* hybridization

A plasmid containing Ku80 full-length cDNA was linearized with Kpn1 restriction enzyme and transcribed with T7 RNA polymerase in the presence of digoxigenin-labeled nucleotides (Roche Applied Science, Indianapolis, IN, USA). Whole-mount *in situ* hybridization was carried out under standard conditions as described elsewhere (34).

Sectioning of embryos

Embryos to be sectioned were fixed as in (34), transferred to a solution of 30% sucrose in PBS and incubated at room temperature for 2 h with gentle mixing. Subsequently, embryos were transferred to PBS containing 15% gelatin for 6 h at 37°C, then transferred to PBS containing 25% gelatin and incubated overnight at 37°C. Single embryos were transferred in PBS containing 25% gelatin to aluminum foil molds and oriented; the gelatin was allowed to set at room temperature for 1 h, then at 4°C for 1 h; and the embryos were stored at −20°C. The gelatin block was mounted on a cryostat chuck using OCT embedding medium (Bayer, Elkhart, IN, USA) and trimmed, and 14 μm sections were cut. Sections were placed on slides (Superfrost Plus, VWR, West Chester, PA, USA) and air dried overnight. Gelatin was removed from slides by incubating in distilled water at 50°C for 15 min and then mounted with a coverslip and aqueous mounting buffer.

Morpholino oligonucleotides

The sequences of the morpholinos (Gene-Tools, LLC, Philomath, OR, USA) are Ku80 MO (5′-TGCTGGCTTCCG-CTCGTGCCGAATT); Ku80 mutMO (5′-TcCTGGgTTCC-cCTgGTGCCcAATT) with lowercase letters representing the 5 nt mismatches; Ku80 MO2 (5′-CATCGCTGCT-GGCTTCCGCTCGT) and zebrafish p53 MO (5′-GCGCCAT-TGCTTTGCAAGAATTG) (35). For microinjection, MOs were diluted to 5 μg/μl in 2× injection buffer (36) and injected into the yolk of 1-cell embryos. Titration of Ku80 MOs determined that up to 10 ng of injected Ku80 MO was not toxic and 5 ng is sufficient to generate a radiosensitive phenotype. Each experiment included both mock-injected (receiving injection buffer alone) and uninjected control groups. In no case were differences seen between mock-injected and uninjected embryos. Each experiment was repeated 2–3 times using at least two different MO doses per experiment. Although the time course of recovery of Ku80 expression was not measured, MOs have previously been shown to attenuate protein expression for 50–65 hpf (26).

mRNA over-expression

The zebrafish Ku80 cDNA was subcloned into the pCS2+ expression vector (37) and sequenced. The resulting construct contained 4 nt of 5′-untranslated sequence, the complete open reading frame and 3′-untranslated sequence extending to the polyA site. This cDNA clone does not contain 5′-untranslated sequence complementary to the Ku80 MO and is, therefore, not recognized by the morpholino. Template plasmid was linearized with NotI restriction enzyme and Ku80 mRNA was transcribed using SP6 RNA polymerase (Message Machine, Ambion Inc., Austin, TX, USA), according to the manufacturer's instructions. Capped mRNAs were purified by phenol-chloroform extractions, dissolved in diethylpyrocarbonate-treated water, and quantified by UV absorbance. Enhanced Green Fluorescent Protein (EGFP) mRNA served as controls for RNA integrity and was injected alone or in combination with Ku80 mRNA or Ku80 MOs.

RESULTS

Sensitivity of the zebrafish embryo to ionizing radiation

To determine the dose-dependent response of zebrafish embryos to radiation, we began by irradiating embryos at the early gastrula stage (6 hpf). At this developmental stage, cells are able to undergo stress-induced apoptosis (18), but have not assumed differentiated cell fates. Thus these cells represent an undifferentiated and uncommitted population at the time of treatment. Gastrula-stage embryos were irradiated at an intermediate dose (150 cGy), allowed to continue development and processed at several stages (12, 18, 24, 30 and 36 hpf) to detect apoptotic cell death by the TUNEL assay (data not shown). We observed a progressive increase in the number of TUNEL-positive cells, as a function of time post-irradiation, at least through 24 hpf, after which increasing pigmentation obscures the signal from the TUNEL reaction (data not shown). Therefore, we chose the 24 hpf endpoint for more detailed analyses. At this developmental stage, most major organ systems have formed, and it is possible to assess the spatial distribution of apoptotic cells relative to distinct anatomical structures. The number of cell divisions intervening between irradiation at 6 hpf and fixation at 24 hpf varies, depending on the tissue, but is no more than two or three (36).

A dose response for embryos irradiated at 6 hpf and assayed at 24 hpf is shown in Figure 1. Mock-irradiated embryos (0 cGy) showed a low level of apoptosis in the head and tail regions, consistent with normal levels of apoptosis observed during development. Although the absolute number of TUNEL-positive cells varies between embryo clutches treated under the same conditions, the relative number of apoptotic cells within a clutch, and in response to experimental manipulation, is consistent among clutches. Thus, the increase in apoptosis with increasing radiation dose shown in Figure 1A and subsequent figures is typical. Exposure to 15 cGy did not significantly change the number of TUNEL-positive cells relative to the background in mock-irradiated embryos of the same clutch (Figure 1B). In contrast, embryos exposed to 50 cGy had a distinct increase in the number of TUNEL-positive cells located in the central nervous system (CNS) (Figure 1C). Although TUNEL staining is seen throughout the CNS, increased staining is most evident in the developing hindbrain and anterior spinal cord (Figure 1, arrows). At higher doses, the number of TUNEL-stained cells increased further. Eventually, cell death reached a level resulting in gross malformation of the head.

The zebrafish diploid genome size is estimated to be 3.4×10^9 bp (38) so that a 15 cGy dose will induce about two DSBs per cell in the embryo [assuming an efficiency of DSB formation in the range of 25 DSB per Gy per 6×10^9 bp (39,40)]. In most systems, a single unrepaired DSB evokes a strong biological response, resulting in cell cycle arrest or apoptosis. The ability of the embryo to survive and grow following this radiation dose provides a strong indication that one or more double-strand break repair pathways are active during zebrafish embryogenesis. Moreover, the absence of ectopic apoptotic cell death at 15 cGy, compared with the large amount at only a 3-fold higher dose, suggests the existence of a threshold below which radiation-induced cell death does not occur. Similar threshold effects have been observed in mammalian embryos during organogenic stages. However, the presence of gross developmental malformations was the only biological endpoint in these experiments [reviewed in (41)]. Additional dose response measurements in this exposure range will be necessary to confirm and quantitatively assess this apparent threshold effect in zebrafish embryos. Regardless, these results led us to pursue and identify the DSB repair pathway that protects embryonic cells from low dose radiation exposure.

Sequence and domain structure of the zebrafish Ku80 gene

The Ku protein, composed of Ku70 and Ku80 subunits, carries out the initial DNA end recognition step in NHEJ, and is well characterized biochemically and genetically in mammalian systems (42). A search of zebrafish genomic and expressed sequence tag (EST) databases identified homologs of both subunits of Ku, as well as most of the mammalian genes in the NHEJ and homologous recombination pathways of DSB repair (data not shown). The *XRCC5* gene, which encodes the Ku80 subunit, was selected for characterization in detail.

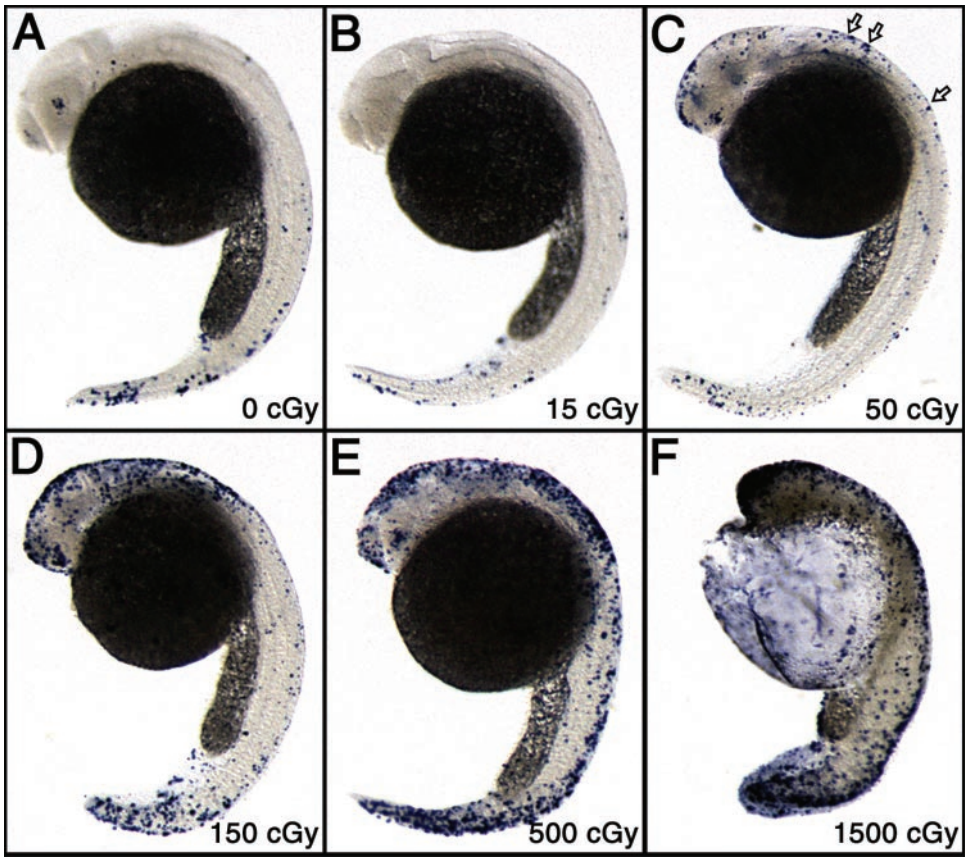

Figure 1. Induction of apoptotic cell death in the developing embryo after exposure to ionizing radiation. (**A–F**) Embryos received the indicated dose of ^{137}Cs gamma radiation at the early gastrula (6 hpf) stage, were allowed to continue development until 24 hpf and were processed to detect apoptotic cells by the TUNEL assay. Anterior is at top left, posterior is toward the bottom and the dark sphere is the yolk cell. Note that low levels of apoptosis occur during normal embryonic development. Arrows in panel C denote marked increase in apoptosis in the hindbrain and anterior spinal cord. Gross malformations (absence of eye, shortening of tail) are seen at higher doses (panels E–F). Embryos shown are from a single experiment and are representative of results obtained in several additional experiments.

A full-length zebrafish Ku80 cDNA clone was isolated from 24 hpf RNA and sequenced (GenBank accession number AY877316). The zebrafish Ku80 cDNA is 2540 nt long and the open reading frame encodes a predicted protein of 727 amino acids. The domain structure of zebrafish Ku80 protein is similar to that of other vertebrate Ku80 and Ku70 proteins (Figure 2A). When compared with Ku80 in other vertebrates, zebrafish Ku80 is most closely related to pufferfish, but has >50% identity to Ku80 in more distantly related mammalian species (Figure 2B, 2C).

Only a single Ku80 mRNA amplification product was identified in RT–PCR analyses using RNA from several developmental stages (Figure 3A). In addition, searches of zebrafish EST and genomic sequence databases failed to identify other zebrafish Ku80 homologs or related genes. Thus, like other vertebrates, including humans, zebrafish appear to have only a single Ku80 gene.

Temporal and spatial expression of zebrafish Ku80 mRNA

Ku80 mRNA is expressed at all stages of embryogenesis examined. Semi-quantitative PCR analysis of Ku80 expression levels during embryonic development detected maternal Ku80 mRNA at the 1-cell stage (Figure 3A), which is before zygotic transcription. Zygotic expression of Ku80 mRNA increased substantially during gastrulation (6 hpf; Figure 3A) and continued through 24, 48 and 72 hpf (Figure 3A and data not shown).

Ku80 mRNA expression becomes spatially restricted during development. Early in embryogenesis, Ku80 mRNA is expressed uniformly among blastomeres at the 2-cell stage (Figure 3B), through gastrulation (6 hpf; Figure 3C) and until the end of somitogenesis (data not shown). By 24 hpf, spatially restricted domains of elevated Ku80 mRNA expression included the developing retina (white arrow; Figure 3D), anterior CNS and otic vesicle (asterisk, Figure 3D). Ku80 mRNA expression was also detectable in the pronephric ducts (open arrows; Figure 3D) and mesenchymal cells located ventrally in the tail. By 48 hpf, specific regions of the anterior CNS continued to express higher levels of Ku80 mRNA (i.e. posterior tectum; black arrow, Figure 3I). Additional domains of Ku80 expression included the pharyngeal mesenchyme at 48 hpf (open triangle; Figure 3I) and the proctodeum at 72 hpf (open arrow; Figure 3J).

To determine more precisely which cells in the CNS and retina express Ku80 mRNA at 24hpf, we examined embryos in flat mount or histological sections (Figure 3E–H). Domains of Ku80 mRNA expression included retinal ganglion cell progenitors and cells surrounding each brain ventricle

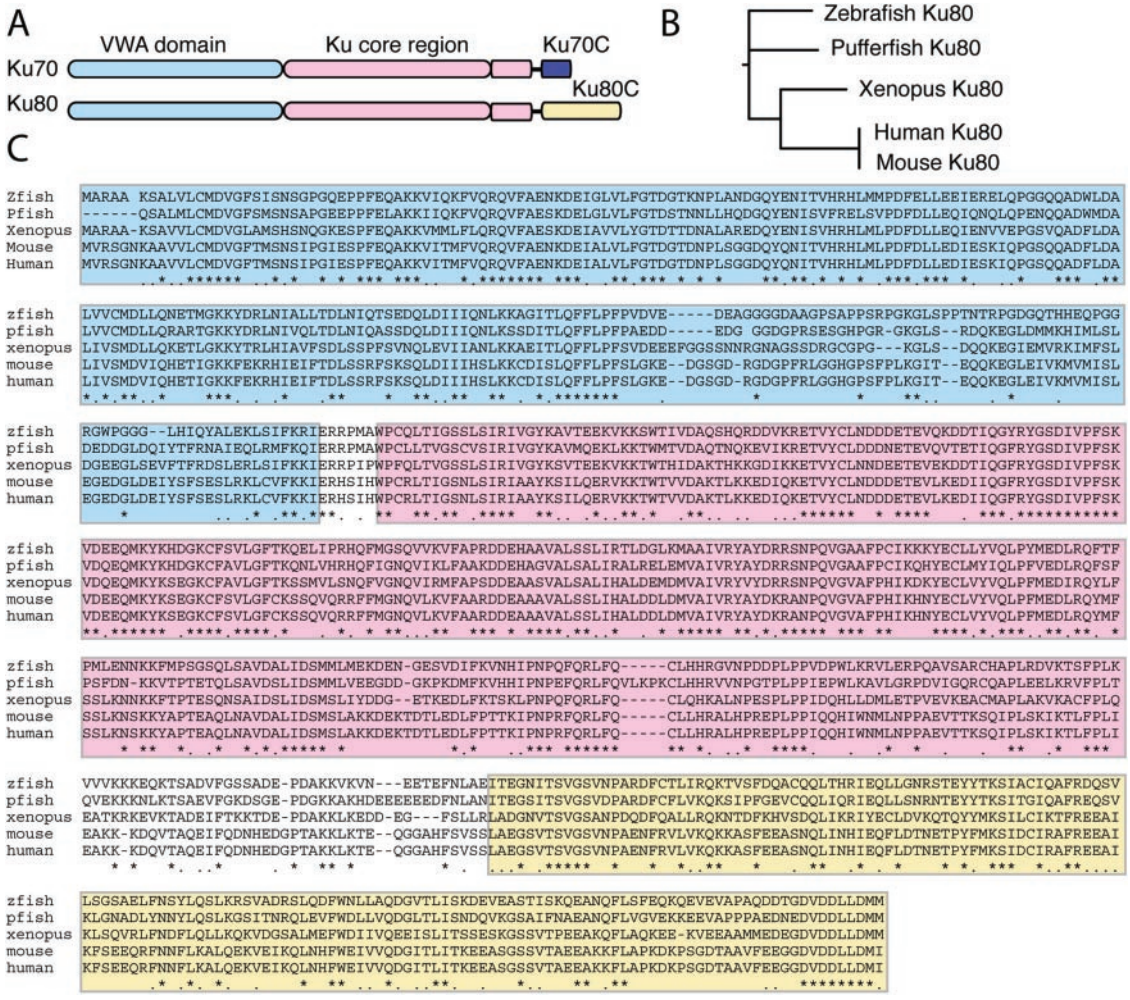

Figure 2. Primary sequence and comparative analysis of zebrafish Ku80 protein. (**A**) Overall domain organization of eukaryotic Ku subunits. Ku70 and Ku80 have identical folds throughout much of their length (61). A von Willebrand Factor type A domain (VWA) domain is present at the N-terminus. The Ku core region, composed of a central β-barrel and small adjacent 'arm' domain, is present in all known eukaryotic and prokaryotic Ku homologs and forms the sliding clamp that encircles the DNA duplex. Small C-terminal domains mediate subunit-specific functions. (**B**) Phylogenetic tree showing relationship of zebrafish Ku80 to Ku80 in other vertebrates. (**C**) Sequence alignment of Ku80 proteins. Amino acid sequence is shown in the single-letter code. Asterisks denote identity; dots denote similarity shared among five vertebrate Ku80 proteins. Shown are zebrafish (zfish), pufferfish (pfish), *Xenopus*, mouse and human.

(Figure 3E–G). Comparison of Ku80 mRNA expression (Figure 3G) and the location of mitotic cells expressing phosphorylated histone H3 (Figure 3H) (43,44) illustrates that domains of Ku80 expression correspond closely with proliferative regions of the CNS.

Ku80 function is required for radioprotection during embryogenesis

To investigate Ku80 function during embryonic development, we injected 5 ng of Ku80 morpholino oligonucleotide (Ku80 MO) at the 1-cell stage to suppress translation of endogenous Ku80 mRNA (26). Control and microinjected embryos were irradiated at the early gastrula stage (6 hpf), allowed to continue development and assayed for apoptotic cell death by TUNEL staining at 24 hpf. Embryos that received a combination of Ku80 MO and radiation showed a dramatic increase in the number of TUNEL-positive cells compared with embryos that received radiation alone (Figure 4). At 24 hpf, TUNEL-positive cells were seen primarily in the CNS, suggesting that Ku80 function is necessary between 6 and 24 hpf to protect prospective neural ectoderm cells from the effects of low dose irradiation. Sometimes embryos receiving a combination of Ku80 MO and radiation also showed abnormal gross brain morphology, probably a secondary consequence of increased cell death, but this was variable between clutches.

TUNEL staining of the CNS in Figure 4 does not appear to be confined to the small region, lining the ventricle, where maximum levels of Ku80 are expressed (Figure 2). It is possible that TUNEL-positive cells are the progeny of cells located on the ventricular surface, a proliferative zone in the brain and source of migratory cells that differentiate into neurons (45). Lineage tracing will be important to definitively establish the relationship between the cells containing high levels of Ku80 mRNA in normal embryos and radiosensitive cells in MO-treated embryos.

Control experiments demonstrate the specificity of the radiosensitive phenotype. Injection of a mutant Ku80 MO, bearing a 5 bp sequence mismatch, did not lead to radiosensitivity. In addition, neither the Ku80 MO nor the mutant Ku80

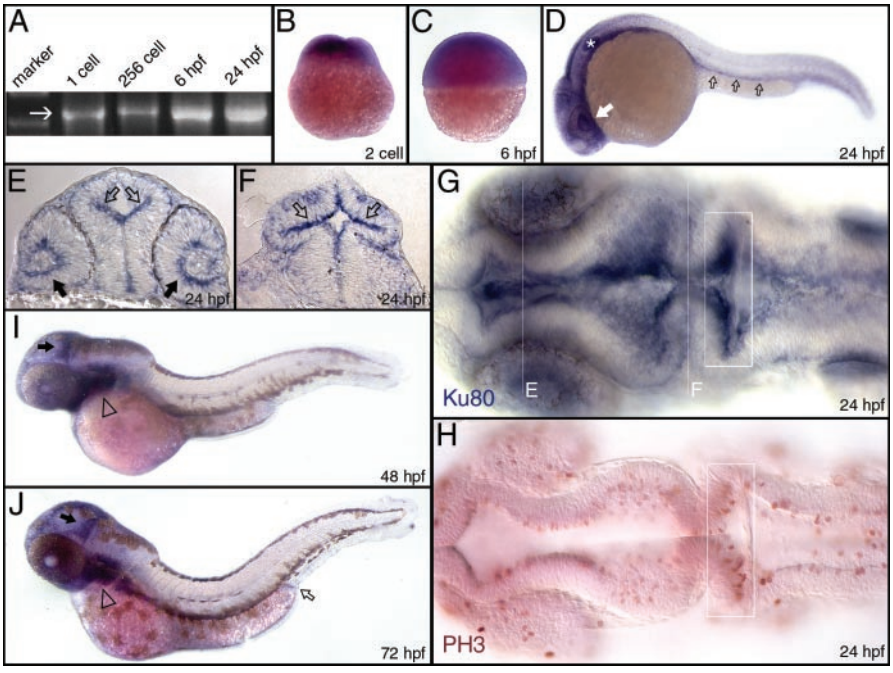

Figure 3. Expression of zebrafish Ku80 mRNA during embryogenesis. (**A**) Semi-quantitative RT–PCR analysis of Ku80 mRNA levels at the indicated developmental stages. (**B–D**) Whole-mount *in situ* hybridization to detect spatial expression of Ku80 mRNA. Ku 80 mRNA is uniform among blastomeres at the 2-cell (B) and early gastrula (6 hpf, C) stages. (D) At the Prim-5 stage (24 hpf) Ku80 mRNA accumulates in the developing retina (white arrow), otic vesicle (asterisk) and pronephric ducts (open arrows). Transverse sections of the midbrain (**E**) and isthmus (**F**) of the embryo shown in (**G**). Ku80 mRNA is expressed in cells along the ventricular surface (open arrows) and in retinal ganglion cells (black arrows). (G) Flat mount of 24 hpf embryo showing Ku80 mRNA expression in cells lining the brain ventricles. Vertical lines denote level of sections shown in (E) and (F). (**H**) Flat mount of 24 hpf embryos stained for phopho-Histone H3 (PH3) to identify cells in the G2/M transition of mitosis. PH3 positive cells (labeled in red) are located along the ventricular surface of the brain, similar to the pattern of Ku80 mRNA expression (compare white boxes in panels G and H). (**I**) At 48 hpf, Ku80 mRNA accumulates in pharyngeal mesenchyme (open triangles) and posterior tectum (filled arrows). (**J**) At 72 hpf, Ku80 mRNA is also detected in the proctodeum (open arrow). (D, I, and J) Lateral views with anterior to the left and dorsal to the top; (G and H) dorsal views with anterior to left.

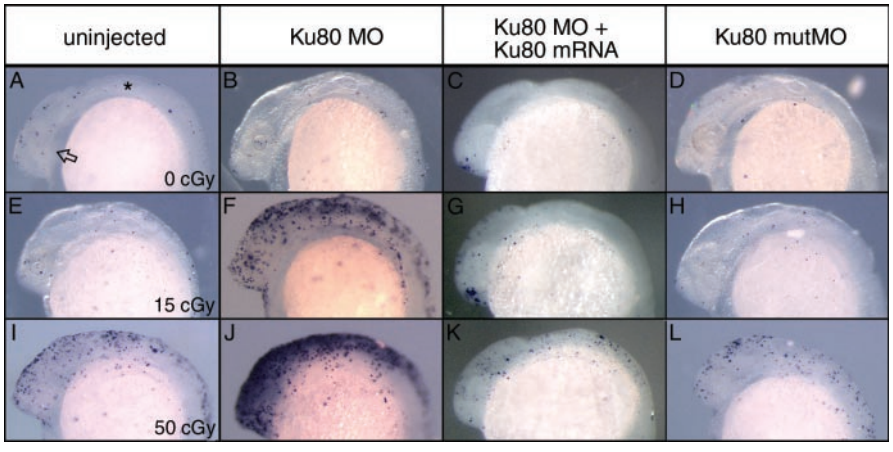

Figure 4. Ku80 is required for radioprotection during embryogenesis. Embryos were exposed to the indicated doses of radiation (cGy) at 6 hpf, allowed to continue development and processed at 24 hpf to detect apoptosis by the TUNEL assay. (**A, E, I**) Uninjected embryos. (**B, F, J**) Embryos microinjected at 1-cell stage with ~5 ng Ku80 morpholino oligonucleotide (Ku80 MO). (**C, G, K**) Embryos microinjected with a combination of ~5 ng Ku80 MO and 200 ng of *in vitro*-transcribed Ku80 mRNA, prepared as described in Materials and Methods. The Ku80 MO is targeted against a 5′-untranslated sequence that is not present in the *in vitro*-synthesized Ku80 mRNA used for phenotypic rescue (18). (**D, H, L**) Embryos microinjected with 5 ng Ku80 mutant morpholino oligonucleotide (mutMO). All panels show lateral views of the anterior portion of embryo at 24 hpf. The asterisk denotes the otic vesicle; the open arrow denotes the retina. All panels are from the same experiment.

MO led to any increase in TUNEL-positive cells in the absence of radiation. A similar radiosensitive phenotype was obtained using a second Ku80 MO. The effect of Ku80 MO was gene specific, as co-injection of Ku80 MO with Ku80 mRNA, not recognized by Ku80 MO, rescued the radiosensitive phenotype (Figure 4). Co-injection of GFP mRNA and Ku80 MO did not rescue the radiosensitivity phenotype (data not shown).

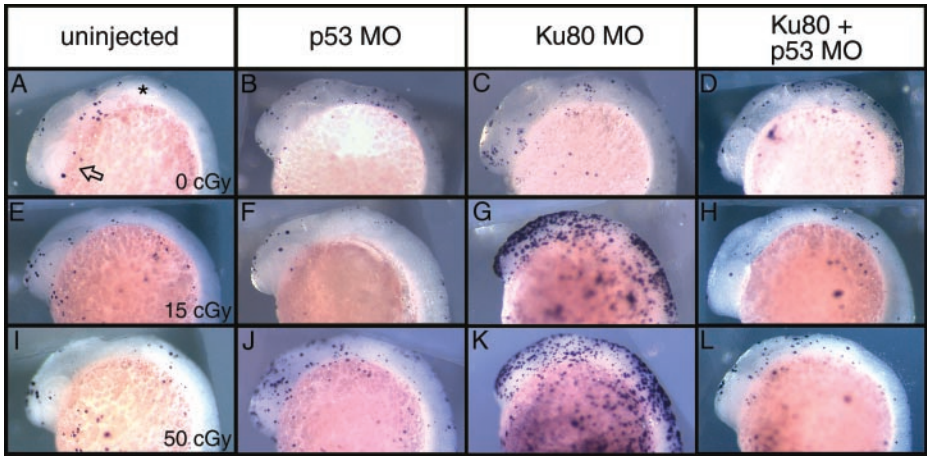

Figure 5. p53-mediated apoptosis in radiosensitive Ku80 morphants. Experimental design as in Figure 4. (**A, E, I**) Uninjected embryos. (**B, F, J**) Embryos injected at the 1-cell stage with ~5 ng p53 morpholino oligonucleotide (P53 MO). (**C, G, K**) Embryos injected at the 1-cell stage with ~5 ng Ku80 MO. (**D, H, L**) Embryos injected at the 1-cell stage with 5 ng Ku80 MO and 5 ng p53 MO. Orientation of embryos and labeling as in Figure 4. All panels are from the same experiment.

The tumor suppressor p53 is essential for DNA damage-induced apoptosis in many systems [reviewed in (46)]. To determine whether increased radiosensitivity in Ku80 MO-treated embryos was attributable to p53-dependent apoptosis, we co-injected Ku80 MO and a p53 morpholino oligonucleotide [p53 MO (35)] to reduce both p53 and Ku80 gene functions. Co-injection of p53 MO completely suppressed the Ku80 MO-induced increase in apoptotic cell death following irradiation (Figure 5). Co-injection of p53 MO partially reversed the morphologic phenotype brought on by irradiation of Ku80 MO injection and this is probably a consequence of reduced apoptotic cell death. For example, the embryo in Figure 5H had normal gross morphology, whereas the embryo in Figure 5G had a reduced head size phenotype.

The p53 tumor suppressor protein functions primarily as a transducer of DNA damage signals in cells of higher eukaryotes. Thus, the ability of co-injected p53 MO to suppress the effect of Ku80 MO demonstrates that increased apoptosis in Ku80 MO-treated and irradiated embryos is likely to be a direct response to radiation-induced DNA damage. The p53 gene is a component of several signaling pathways, and we have not yet examined which of these is essential for DNA damage-induced cell death in the early embryo.

In the absence of radiation, Ku80 MO-treated embryos developed normally, were viable for at least one year and were fertile (data not shown). Although subtle effects of Ku80 deficiency on genome stability or reproductive fitness cannot be excluded, it appears that the primary function of Ku80 is to mitigate the effects of radiation exposure, and that it is dispensable for normal embryonic development.

DISCUSSION

We have characterized the mRNA expression pattern and determined the requirement for zebrafish Ku80 gene function during vertebrate embryogenesis. We find that apoptosis, as measured by the TUNEL assay, provides a rapid, quantifiable endpoint for measuring radiation injury in the dose range of 15–150 cGy. Our results indicate a central role for Ku80 in effecting the decision between cell survival and radiation-induced cell death.

DNA repair by the NHEJ repair pathway in vertebrates requires at least five gene products: Ku80 (XRCC5), Ku70 (G22P1), DNA ligase IV (LIG4), XRCC4 and the DNA-dependent protein kinase catalytic subunit (PRKDC) [reviewed in (2)]. Putative orthologs for each of these can be identified in the zebrafish EST database (data not shown). The presence of these genes, together with the functional characterization of the Ku80 gene described here, suggest that an intact functional nonhomologous end joining pathway probably operates in the zebrafish.

Comparison with other vertebrate Ku proteins (Figure 1) shows that the predicted zebrafish Ku80 polypeptide contains all the domains present in other Ku proteins, including a central Ku core region that mediates dimerization and DNA binding, an N-terminal VWA domain (47) that mediates additional DNA contacts and a Ku80-specific C-terminal domain that mediates protein–protein interactions (48–50). Several short runs of amino acids are nearly 100% conserved among vertebrate Ku80 genes and are candidate regions to mediate conserved interactions with other macromolecules. For example, a conserved octapeptide sequence at the extreme C-terminus has been shown experimentally to mediate interaction of human Ku80 with the DNA-dependent protein kinase catalytic subunit (48).

Although DNA repair proteins are often considered to be housekeeping enzymes, zebrafish Ku80 mRNA has an unexpected tissue-specific pattern of accumulation during organogenesis and later stages of development. Spatially and temporally restricted accumulation of Ku80 may serve to protect specific populations or domains of rapidly proliferating cells, which also contain organ-specific progenitor cells. Several regions of the embryo accumulate higher levels of Ku80 mRNA and meet this criterion, including the ventricular surfaces of the CNS and retinal ganglion cells surrounding the lens (51).

The phenotype resulting from Ku80 deficiency becomes apparent only when embryos are exposed to an external source of DNA damage. These embryos are more sensitive to radiation-induced apoptosis than control embryos, with most TUNEL-positive cells located in the developing CNS. This apoptosis is p53 dependent, indicating that radiation-induced DNA damage is the primary trigger (Figure 5).

Our results demonstrating an epistatic relationship between p53 and an NHEJ gene recapitulate data obtained from mouse models. In the mouse, homozygous null mutation of a different NHEJ gene, Lig4, is embryonically lethal (52). Post-mitotic neurons die by apoptosis, even in the absence of radiation, apparently because of sensitivity to endogenous DNA damaging agents (i.e. reactive oxygen species generated by oxidative metabolism). This early apoptosis is suppressed in a p53-/- background, just as radiation-induced apoptosis in the Ku80-injected zebrafish is suppressed by the p53 MO (53).

A Ku80 and p53 double knockout mouse has also been characterized (54). Results cannot be directly compared to those here, because the Ku80 single knockout mouse and the Ku80/p53 double knockout mouse were not directly compared with respect to radiation sensitivity or apoptosis. However, loss of p53 synergized with loss of Ku80 to promote early tumorigenesis, suggesting indirectly that loss of p53 allowed survival of cells with unrepaired DSBs that otherwise would have been eliminated. Thus, the overall conclusions of the study are consistent with the findings reported here.

In vertebrates, homologous recombination functions as an alternative pathway for repair of radiation-induced DSBs. The role of HR is more difficult to investigate genetically than NHEJ because all but one of the genes in the HR pathway are also required for somatic cell viability in the absence of radiation [reviewed in (3)]. To assess the role of HR, we have begun to test MOs directed against the one component of the HR pathway that is nonessential for cell growth, Rad54. Although these preliminary experiments were not exhaustive, neither of the two MOs tested had any effect on embryogenesis, viability or cell survival, with or without radiation (data not shown).

In contrast, our data demonstrate a requirement of Ku80 function for embryonic radioresistance. Our results are reproducible among multiple embryo clutches tested for each experiment and completely consistent within a clutch. Laboratory strains of zebrafish are not as inbred as other models such as the mouse. To minimize the impact of genetic variation, each experiment used offspring derived from a single breeding pair of adults. Mock-irradiated, mock-injected and uninjected control groups were included in every experiment (see Materials and Methods).

The findings that Ku80 function is necessary for radioprotection during embryogenesis is relevant to human health, where the consequences of radiation exposure to brain development are well documented (5). The dose range of 15–150 cGy, used in the majority of our experiments, is equivalent to 7.5–75 cGy in human, which has a 2-fold larger genome. This corresponds with the range of prenatal exposures that resulted in sharply increased risk of microcephaly, severe mental retardation, lower IQ and seizure disorders in the Japanese atomic bomb *in utero* cohort (55–57). Recently, there has been a renewal of interest in the consequences of low dose radiation exposure of sensitive populations (58,59), which may include children and pregnant women. More intensive use of medical imaging procedures, especially repeated spiral CT scans in pediatric patients, has also engendered health concerns (60).

The established framework for understanding the effects of radiation on the vertebrate embryo posits that radiation-induced malformations in the brain and other organs are induced by exposure during a 'critical period' during organogenesis and reflect an inherent bias toward cellular self-elimination rather than DNA repair, cell survival and altered developmental programs. Present results in the zebrafish model challenge this assumption and suggest the operation of a dynamic process, where spatially and temporally regulated expression of DSB repair genes protects against acute effects of low dose radiation injury and promotes cell survival. The ability to tolerate and repair DNA damage may be two edged: by promoting cellular survival, DNA repair may reduce the incidence of radiation-induced developmental malformations, while at the same time increasing the risk of delayed effects attributable to radiation-induced mutations and genome instability.

ACKNOWLEDGEMENTS

We thank Dr B. Yuan and the MCG Transgenic Zebrafish Core Facility for embryo production, Dr L. McCluskey for cryotome use, Mr Sammy Navarre for advice and support, Drs J. Hardin and S. Lin for stimulating initial interest in the zebrafish as a radiobiological model, Dr P. Chang (University of Singapore) for providing an independent clone of zebrafish Ku80, and members of our laboratories for critical reading of the manuscript. Open Access publication charges and support for this work were provided by grant award DE-FG02-03ER63649 from the U.S. Department of Energy Low Dose Radiation Research Program.

Conflict of interest statement. None declared.

REFERENCES

1. Ward,J.F. (1995) Radiation mutagenesis: the initial DNA lesions responsible. *Radiat. Res.*, **142**, 362–368.
2. Collis,S.J., Deweese,T.L., Jeggo,P.A. and Parker,A.R. (2005) The life and death of DNA-PK. *Oncogene*, **24**, 949–961.
3. Sonoda,E., Takata,M., Yamashita,Y.M., Morrison,C. and Takeda,S. (2001) Homologous DNA recombination in vertebrate cells. *Proc. Natl Acad. Sci. USA*, **98**, 8388–8394.
4. Zhivotovsky,B. and Kroemer,G. (2004) Apoptosis and genomic instability. *Nat. Rev. Mol. Cell Biol.*, **5**, 752–762.
5. Streffer,C., Shore,R., Konermann,G., Meadows,A., Uma Devi,P., Preston,J., Holm,L.E., Stather,J., Mabuchi,K. and Withers,H.R. (2003) Biological effects after prenatal irradiation (embryo and fetus). A report of the International Commission on Radiological Protection. *Ann. ICRP*, **33**, 5–206.
6. Russell,L.B. and Russell,W.L. (1954) Pathways of radiation effects in the mother and the embryo. *Cold Spring Harb. Symp. Quant. Biol.*, **19**, 50–59.
7. Obasaju,M.F., Wiley,L.M., Oudiz,D.J., Miller,L., Samuels,S.J., Chang,R.J. and Overstreet,J.W. (1988) An assay using embryo aggregation chimeras for the detection of nonlethal changes in X-irradiated mouse preimplantation embryos. *Radiat. Res.*, **113**, 289–299.
8. Wiley,L.M., Raabe,O.G., Khan,R. and Straume,T. (1994) Radiosensitive target in the early mouse embryo exposed to very low doses of ionizing radiation. *Mutat. Res.*, **309**, 83–92.
9. Dekaban,A.S. (1968) Abnormalities in children exposed to x-radiation during various stages of gestation: tentative timetable of radiation injury to the human fetus. I. *J. Nucl. Med.*, **9**, 471–477.
10. Upton,A.C., Odell,T.T.,Jr and Sniffen,E.P. (1960) Influence of age at time of irradiation on induction of leukemia and ovarian tumors in RF mice. *Proc. Soc. Exp. Biol. Med.*, **104**, 769–772.
11. Sasaki,S., Kasuga,T., Sato,F. and Kawashima,N. (1978) Late effects of fetal mice X-irradiated at middle or late intrauterine stage. *Gann*, **69**, 167–177.
12. Norimura,T., Nomoto,S., Katsuki,M., Gondo,Y. and Kondo,S. (1996) p53-dependent apoptosis suppresses radiation-induced teratogenesis. *Nat. Med.*, **2**, 577–580.
13. Wang,B., Ohyama,H., Haginoya,K., Odaka,T., Yamada,T. and Hayata,I. (2000) Prenatal radiation-induced limb defects mediated by Trp53-dependent apoptosis in mice. *Radiat. Res.*, **154**, 673–679.

14. Shimura,T., Toyoshima,M., Taga,M., Shiraishi,K., Uematsu,N., Inoue,M. and Niwa,O. (2002) The novel surveillance mechanism of the Trp53-dependent s-phase checkpoint ensures chromosome damage repair and preimplantation-stage development of mouse embryos fertilized with x-irradiated sperm. *Radiat. Res.*, **158**, 735–742.
15. Hensey,C. and Gautier,J. (1997) A developmental timer that regulates apoptosis at the onset of gastrulation. *Mech. Dev.*, **69**, 183–195.
16. Anderson,J.A., Lewellyn,A.L. and Maller,J.L. (1997) Ionizing radiation induces apoptosis and elevates cyclin A1-Cdk2 activity before but not after the midblastula transition in Xenopus. *Mol. Biol. Cell*, **8**, 1195–1206.
17. Stack,J.H. and Newport,J.W. (1997) Developmentally regulated activation of apoptosis early in Xenopus gastrulation results in cyclin A degradation during interphase of the cell cycle. *Development*, **124**, 3185–3195.
18. Ikegami,R., Hunter,P. and Yager,T.D. (1999) Developmental activation of the capability to undergo checkpoint-induced apoptosis in the early zebrafish embryo. *Dev. Biol.*, **209**, 409–433.
19. Uma Devi,P. and Hossain,M. (2000) Induction of solid tumours in the Swiss albino mouse by low-dose foetal irradiation. *Int. J. Radiat. Biol.*, **76**, 95–99.
20. Giles,D., Hewitt,D., Stewart,A. and Webb,J. (1956) Malignant disease in childhood and diagnostic irradiation in utero. *Lancet*, **271**, 447.
21. Stewart,A. and Kneale,G.W. (1968) Changes in the cancer risk associated with obstetric radiography. *Lancet*, **1**, 104–107.
22. Stewart,A., Webb,J. and Hewitt,D. (1958) A survey of childhood malignancies. *Br. Med. J.*, **30**, 1495–1508.
23. Doll,R. and Wakeford,R. (1997) Risk of childhood cancer from fetal irradiation. *Br. Med. J.*, **70**, 130–139.
24. McAleer,M.F., Davidson,C., Davidson,W.R., Yentzer,B., Farber,S.A., Rodeck,U. and Dicker,A.P. (2005) Novel use of zebrafish as a vertebrate model to screen radiation protectors and sensitizers. *Int. J. Radiat. Oncol. Biol. Phys.*, **61**, 10–13.
25. Amatruda,J.F., Shepard,J.L., Stern,H.M. and Zon,L.I. (2002) Zebrafish as a cancer model system. *Cancer Cell*, **1**, 229–231.
26. Nasevicius,A. and Ekker,S.C. (2000) Effective targeted gene 'knockdown' in zebrafish. *Nat. Genet.*, **26**, 216–220.
27. Getts,R.C. and Stamato,T.D. (1994) Absence of a Ku-like DNA end binding activity in the xrs double-strand DNA repair-deficient mutant. *J. Biol. Chem.*, **269**, 15981–15984.
28. Smider,V., Rathmell,W.K., Lieber,M.R. and Chu,G. (1994) Restoration of X-ray resistance and V(D)J recombination in mutant cells by Ku cDNA. *Science*, **266**, 288–291.
29. Taccioli,G.E., Gottlieb,T.M., Blunt,T., Priestley,A., Demengeot,J., Mizuta,R., Lehmann,A.R., Alt,F.W., Jackson,S.P. and Jeggo,P.A. (1994) Ku80: product of the XRCC5 gene and its role in DNA repair and V(D)J recombination. *Science*, **265**, 1442–1445.
30. Khanna,K.K. and Jackson,S.P. (2001) DNA double-strand breaks: signaling, repair and the cancer connection. *Nat. Genet.*, **27**, 247–254.
31. Westerfield,M. (1995) *The Zebrafish Book*. 3rd ed. University of Oregon Press, Eugene, OR.
32. Kimmel,C.B., Ballard,W.W., Kimmel,S.R., Ullmann,B. and Schilling,T.F. (1995) Stages of embryonic development of the zebrafish. *Dev. Dyn.*, **203**, 253–310.
33. Kozlowski,D.J., Whitfield,T.T., Hukriede,N.A., Lam,W.K. and Weinberg,E.S. (2005) The zebrafish dog-eared mutation disrupts eya1, a gene required for cell survival and differentiation in the inner ear and lateral line. *Dev. Biol.*, **277**, 27–41.
34. Thisse,C., Thisse,B., Schilling,T.F. and Postlethwait,J.H. (1993) Structure of the zebrafish snail 1 gene and its expression in wild-type, spadetail and no tail mutant embryos. *Development*, **119**, 1203–1215.
35. Langheinrich,U., Hennen,E., Stott,G. and Vacun,G. (2002) Zebrafish as a model organism for the identification and characterization of drugs and genes affecting p53 signaling. *Curr. Biol.*, **12**, 2023–2028.
36. Kozlowski,D.J., Murakami,T., Ho,R.K. and Weinberg,E.S. (1997) Regional cell movement and tissue patterning in the zebrafish embryo revealed by fate mapping with caged fluorescein. *Biochem. Cell Biol.*, **75**, 551–562.
37. Turner,D.L. and Weintraub,H. (1994) Expression of achaete-scute homolog 3 in Xenopus embryos converts ectodermal cells to a neural fate. *Genes Dev.*, **8**, 1434–1447.
38. Hinegardner,R. and Rosen,D.E. (1972) Cellular DNA content and the evolution of teleostean fishes. *Am. Nat.*, **106**, 621–644.
39. Iliakis,G.E., Cicilioni,O. and Metzger,L. (1991) Measurement of DNA double-strand breaks in CHO cells at various stages of the cell cycle using pulsed field gel electrophoresis: calibration by means of 125I decay. *Int. J. Radiat. Biol.*, **59**, 343–357.
40. Ruiz de Almodovar,J.M., Steel,G.G., Whitaker,S.J. and McMillan,T.J. (1994) A comparison of methods for calculating DNA double-strand break induction frequency in mammalian cells by pulsed-field gel electrophoresis. *Int. J. Radiat. Biol.*, **65**, 641–649.
41. OECD (1988), *The Biological Basis for the Control of Prenatal Irradiation*. Organization for Economic Cooperation and Development, Paris.
42. Dynan,W.S. and Yoo,S. (1998) Interaction of Ku protein and DNA-dependent protein kinase catalytic subunit with nucleic acids. *Nucleic Acids Res.*, **26**, 1551–1559.
43. Anton,M., Horky,M., Kuchtickova,S., Vojtesek,B. and Blaha,O. (2004) Immunohistochemical detection of acetylation and phosphorylation of histone H3 in cervical smears. *Ceska Gynekol.*, **69**, 3–6.
44. Song,M.H., Brown,N.L. and Kuwada,J.Y. (2004) The cfy mutation disrupts cell divisions in a stage-dependent manner in zebrafish embryos. *Dev. Biol.*, **276**, 194–206.
45. Lyons,D.A., Guy,A.T. and Clarke,J.D. (2003) Monitoring neural progenitor fate through multiple rounds of division in an intact vertebrate brain. *Development*, **130**, 3427–3436.
46. Shen,Y. and White,E. (2001) p53-dependent apoptosis pathways. *Adv. Cancer Res.*, **82**, 55–84.
47. Aravind,L. and Koonin,E.V. (2001) Prokaryotic homologs of the eukaryotic DNA-end-binding protein Ku, novel domains in the Ku protein and prediction of a prokaryotic double-strand break repair system. *Genome Res.*, **11**, 1365–1374.
48. Singleton,B.K., Torres-Arzayus,M.I., Rottinghaus,S.T., Taccioli,G.E. and Jeggo,P.A. (1999) The C terminus of Ku80 activates the DNA-dependent protein kinase catalytic subunit. *Mol. Cell Biol.*, **19**, 3267–3277.
49. Woodard,R.L., Lee,K.J., Huang,J. and Dynan,W.S. (2001) Distinct roles for Ku protein in transcriptional reinitiation and DNA repair. *J. Biol. Chem.*, **276**, 15423–15433.
50. Mo,X. and Dynan,W.S. (2002) Subnuclear localization of Ku protein: functional association with RNA polymerase II elongation sites. *Mol. Cell. Biol.*, **22**, 8088–8099.
51. Wullimann,M.F. and Knipp,S. (2000) Proliferation pattern changes in the zebrafish brain from embryonic through early postembryonic stages. *Anat. Embryol. (Berl.)*, **202**, 385–400.
52. Barnes,D.E., Stamp,G., Rosewell,I., Denzel,A. and Lindahl,T. (1998) Targeted disruption of the gene encoding DNA ligase IV leads to lethality in embryonic mice. *Curr. Biol.*, **8**, 1395–1398.
53. Frank,K.M., Sharpless,N.E., Gao,Y., Sekiguchi,J.M., Ferguson,D.O., Zhu,C., Manis,J.P., Horner,J., DePinho,R.A. and Alt,F.W. (2000) DNA ligase IV deficiency in mice leads to defective neurogenesis and embryonic lethality via the p53 pathway. *Mol. Cell*, **5**, 993–1002.
54. Difilippantonio,M.J., Zhu,J., Chen,H.T., Meffre,E., Nussenzweig,M.C., Max,E.E., Ried,T. and Nussenzweig,A. (2000) DNA repair protein Ku80 suppresses chromosomal aberrations and malignant transformation. *Nature*, **404**, 510–514.
55. Shimizu,Y., Kato,H., Schull,W.J., Preston,D.L., Fujita,S. and Pierce,D.A. (1989) Studies of the mortality of A-bomb survivors. 9. Mortality, 1950–1985: Part 1. Comparison of risk coefficients for site-specific cancer mortality based on the DS86 and T65DR shielded kerma and organ doses. *Radiat. Res.*, **118**, 502–524.
56. Thompson,D.E., Mabuchi,K., Ron,E., Soda,M., Tokunaga,M., Ochikubo,S., Sugimoto,S., Ikeda,T., Terasaki,M. and Izumi,S. (1994) Cancer incidence in atomic bomb survivors. Part II. Solid tumors, 1958–1987. *Radiat. Res.*, **137**, S17–S67.
57. UNSCEAR (2000) The United Nations Scientific Committee on the Effects of Atomic Radiation. *Health Phys.*, **79**, 314.
58. Brooks,A.L. (2003) Developing a scientific basis for radiation risk estimates: goal of the DOE low dose research program. *Health Phys.*, **85**, 85–93.
59. Coleman,C.N., Stone,H.B., Moulder,J.E. and Pellmar,T.C. (2004) Medicine. Modulation of radiation injury. *Science*, **304**, 693–694.
60. Hall,E.J. (2002) Lessons we have learned from our children: cancer risks from diagnostic radiology. *Pediatr. Radiol.*, **32**, 700–706.
61. Walker,J.R., Corpina,R.A. and Goldberg,J. (2001) Structure of the Ku heterodimer bound to DNA and its implications for double-strand break repair. *Nature*, **412**, 607–614.